JOURNAL OF OPTOELECTRONICS AND ADVANCED MATERIALS, Vol. 11, No. 1, January 2009, p. 76 - 82

The effects of annealing treatment in oxygen ambient on $Ni/Al_{0.09}Ga_{0.91}N$ UV photodetectors

L. S. CHUAH*, Z. HASSAN, H. ABU HASSAN
Nano-Optoelectronics Research and Technology Laboratory
School of Physics, Universiti Sains Malaysia, 11800 Minden, Penang, Malaysia.

To date, no approaches have been reported on the effects of annealing treatment in oxygen ambient on $Ni/Al_{0.09}Ga_{0.91}N$ metal-semiconductor-metal (MSM) photodiodes. In this work, unintentionally doped n-type $Al_{0.09}Ga_{0.91}N$ samples were grown by radio frequency (RF) nitrogen plasma-assisted molecular beam epitaxy (MBE) on (111) silicon substrates. High temperature grown AlN (about 200 nm) was used as a buffer layer. MSM photodiode was fabricated on the AlGaN samples with a nickel layer as transparent coplanar Schottky contact. The $Ni/Al_{0.09}Ga_{0.91}N$ samples were annealed at a range of temperatures starting from 400 °C to 700 °C in flowing oxygen by using a tube furnace. The effect of post annealing in oxygen ambient on the electrical properties of Ni/AlGaN is studied by current-voltage (I-V) measurement. We have measured Schottky barrier heights (SBHs) and junction ideality factor (n) straight on the MSM photodiodes. It was found that dark current of the detector became significantly smaller after annealing. With a 10 V applied bias, it was found that we can achieve a photocurrent to dark current contrast ratio of 12 from the photodetectors with 600 ºC annealed Ni contacts. The surface roughness of contacts has been monitored by atomic force microscopy (AFM), and scanning electron microscopy (SEM).

(Received August 6, 2008; accepted January 21, 2009)

Keywords: Dark current, Metal-semiconductor-metal photodiodes, Si(111); AlGaN, UV photodetector

1. Introduction

Apart from the important discovery of blue and violet semiconductor lasers and light emitting diodes based on GaN, another important device for optoelectronic applications is a photodetector. GaN are ideal for the fabrication of high responsivity and visible plumes detection, flame sensing, engine control, solar UV monitoring, source calibration, UV astronomy, and secure blind ultraviolet (UV) detectors due to its unique properties such as wide and direct band gap, high absorption coefficients, and sharper cutoff of the wave-length detection [1]. Photo-detectors operating in the UV and with a visible-blind behavior have drawn great attention in recent years, with a number of applications in both civil and military industries which include missile space to space communications.

On the other hand, by varying the AlN molar fraction in $Al_xGa_{1-x}N$, the band gap of $Al_xGa_{1-x}N$ can be altered accordingly, which in turn provide flexibility to the selection of detection region of the light spectrum in photodetector applications. Moreover, the key advantage of III-V nitrides detectors over competing devices based on semiconductors with smaller band gaps is the long wavelength response cut off, which is directly related to the band gap of the material in the active region and thus, does not require external filters. Unlike wide band gap photodetector, the front surface of a vacuum ultraviolet (VUV) Si photodiode is coated with filter materials to limit the sensitivity of the silicon to a much narrower band in the VUV because one significant shortcoming of Si photodiodes for certain VUV applications is the inherent broadband response extending from X-rays to the near infrared, which is undesirable.

For GaN or AlGaN based photodetectors, the region of detection correspond to the UV part of the solar spectrum. A visible blind or UV photodetectors are normally GaN-based detectors while for the more advanced role which is better known as solar-blind photodetection, AlGaN is normally employed where it is used for the fabrication of this so-called solar-blind photodetector. In UV detector applications, the meaning of a solar-blind photodetector is a device which detects the wavelength in the UV region of the spectrum with the presence of solar radiation.

Among various kinds of photodetectors, there is a keen interest in developing photodetectors in the form of metal-semiconductor-metal (MSM) structure due to reasons like fabrication simplicity, low dark currents, small capacitance, large active area for photo detection, fast response, large bandwidth, low noise, and the suitability for the monolithic integration of an optical receiver [2-4]. Normally the structure of an MSM photodiode consisted of two interdigitated Schottky contacts connected back to back. When a bias is applied to the MSM structure, one of the Schottky contacts is forward biased and the other is reverse biased. So, for characterization of MSM structure with I-V measurement, we can only measure the reverse bias part of the detector [4].

In this paper, we have investigated growth of $Al_{0.09}Ga_{0.91}N$ epilayers grown on silicon (111) using Veeco model Gen II MBE system. Also reported is our attempt to fabricate and characterize metal-semiconductor-metal (MSM) photodiode based on these films. The effect of post annealing in oxygen ambient on the electrical properties of Ni/AlGaN is studied by I-V measurement.

2. Experimental details

The film growth has been performed in a MBE system, sample nominally consisted of 0.20 µm low temperature nucleation layer AlN followed by 0.23 µm AlGaN. The Al content of the sample was measured to be 9 % from high resolution XRD (PANalytical X'pert MRD) simulation.

For the wafer cleaning process prior to metallization of the contact metal, the $Al_{0.09}Ga_{0.91}N$ samples were dipped in a 1:20 NH_4OH:H_2O solution for 15 s followed by a 10 s dip in a 1:50 HF:H_2O solution. Then, it was rinsed with distilled water and blown dry with a nitrogen gas blower. The (Ni) Schottky contacts were deposited by thermal evaporation using a metal mask in patterning of the contact structure.

MSM photodiode is a planar device consisting of two fork-shaped interdigitated contacts oppositely laying on the semiconductor surface. These contacts functions as back to back Schottky contacts with fingers width of 230 µm, finger spacing of 400 µm, and the length of each electrode was about 3.3 mm. It consists of 4 fingers at each electrode as shown in Fig. 1.

The fabricated photodiodes were then annealed at temperatures from 400-700 °C in a conventional tube furnace in flowing oxygen environment. The annealing duration for the samples annealed at temperatures from 400 °C to 500 °C was 15 minutes, while the 600 °C samples were annealed for 5 minutes, and 2 minutes for the 700 ºC samples. The effective Schottky barrier heights (SBHs) are deduced from I-V measurement assuming the results can be described by the standard thermionic emission equation. Keithley high-voltage-source-measure-unit model 237-semiconductor parameter analyzer was used for the I-V measurement.

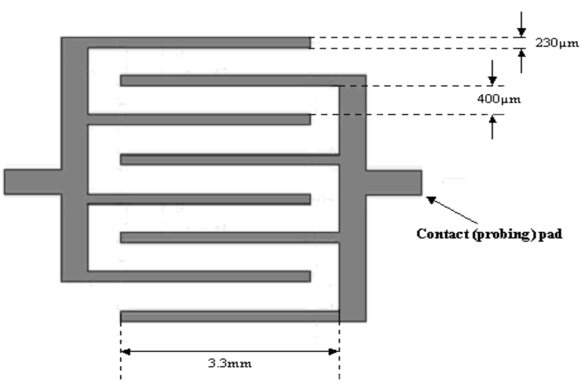

Fig. 1. Schematic diagram of the metal-semiconductor-metal (MSM) structure.

3. Results and discussion

A Schottky contact behaviour can be more closely described by the equation which takes into account the barrier height lowering due to electric field, tunneling effects, the presence of an interfacial layer, and carrier recombination in the space charge region of the metal-semiconductor contact as given by [5-6]

$$I = I_0 \exp(\frac{eV}{nkT})[1-\exp(\frac{-eV}{kT})] \tag{1}$$

where I is the current, I_0 is the saturation current, V is the bias voltage, and n is the ideality factor. The expression for the saturation current, I_0 is

$$I_0 = AA^*T^2 \exp(\frac{-q\Phi_b}{kT}) \tag{2}$$

where A is the Schottky contact area, the theoretical value [7] of A* for GaN is ~ 26.4 $Acm^{-2}K^{-2}$. Here, the theoretical value of A* for $Al_{0.09}Ga_{0.91}N$ can be estimated by using the relation $A^* = 4\pi qm^*k^2/h^3$ where h is Planck's constant and m* is the effective electron mass for AlGaN. As there has not been any references or reported experimental results of the effective mass of electron in AlGaN, therefore m* for $Al_xGa_{1-x}N$ with different x is estimated by a linear interpolation from the theoretical value of $m^* = 0.35\ m_0$ for AlN [8] and $m^* = 0.22\ m_0$ for GaN [9]. Here, m_0 is the free electron mass. From the equation as being mentioned above, A* for $Al_{0.09}Ga_{0.91}N$ is estimated to be ~ 27.9 $Acm^{-2}K^{-2}$. However, it should be noted that a large variation in A* does not have a significant influence on the Φ_B value that is to be determined [10]. Equation (1) can be written in the form of

$$\frac{I\exp(eV/kT)}{\exp(eV/kT)-1} = I_0 \exp(eV/nkT) \tag{3}$$

At $T \leq 370$ K and when $V \leq -0.5$ V, equation (3) can be simplified to [11]

$$I\exp(\frac{eV}{kT}) = I_0 \exp(\frac{eV}{nkT}) \tag{4}$$

$$\ln[I\exp(\frac{eV}{kT})] = \ln I_0 + \frac{eV}{nkT} \tag{5}$$

The plot of $\ln[I\exp(eV/kT)]$ vs V should give a straight line with the slope = e/nkT and y-intercept at $\ln I_0$. Using equation (2), the ideality factor (n) and Schottky barrier height (SBH) were determined by the I-V method.

Figs. 2-6 show the I-V characteristics of Ni/AlGaN photodetectors under dark and illumination conditions. Table 1 summarizes dark and illumination current measured at 10V, as well as the ideality factor and SBH of the samples determined from the I-V measurements. By referring to Table 1, it is found that high temperature annealing in oxygen ambient (600°C and 700°C) resulted in more significant changes to the dark current characteristics compared to the lower temperature annealing treatment. High temperature annealing treatment increased the barrier height as well as reduced the dark current level. For lower annealing temperature (400°C and 500°C), the barrier height for annealed samples (photodiodes) increased. As shown in Fig 2-6, it can be seen that dark currents became significantly smaller after annealing. Such a reduction can again be attributed to the formation of NiO layers since NiO is p-type in nature. As a result, we achieved larger Schottky barrier heights from the thermally annealed samples.

In the literatures, it can been seen that the bi-layer Ni/Au film annealed in oxygen by using photo-CVD would transform the metallic Ni into NiO along with Au grains and amorphous Ni-Ga-O phases [12]. Hence, such the Ni/Au semitransparent contact can be used to form good Schottky contacts with the superior Schottky barrier height. In this study, the $Ni/Al_{0.09}Ga_{0.91}N$ samples were annealed at a range of temperatures in flowing oxygen by using a tube furnace. NiO, which is reported to behave as a p-type semiconductor with nickel vacancies and/or oxygen interstitials, has also been reported as a kind of passivation layer on the AlGaN interface [13].As the annealed temperature increases, the transmittance increases. The increase of transmittance also indicates the formation of NiO. We believe able to achieve excellent photo-current to dark-current contrast ratio from the AlGaN MSM photodetectors, can be attributed to the formation of the transparent NiO in the Ni contacts. It was found that dark current of the detector became significantly smaller after annealing. With a 10V applied bias, it was found that we can achieve a photocurrent to dark current contrast ratio of 12 from the photodetectors with 600 ºC annealed Ni contacts. This could be attributed to the more transparent nature of NiO formed after annealing so that more photons can be absorbed by the underneath AlGaN epitaxial layer. Such an effect should compensate the effect of larger Schottky barrier height. As the annealing temperature was increased to 700 ºC, it was found that we can achieve a photocurrent to dark current contrast ratio of 2, it may be due to the formation of a rough Ni layer surface. Such a rough surface could be increase light scattering losses and thus degraded the film transparency.

On the other hand, for Ni/AlGaN schottky contact, the effect of "surface patches" which originates from surface defects such as dislocations and micropipes with residual oxides may not be neglectable [14]. Postannealing is an effective method to repair the surface patches. However, considering that the annealing temperature is relatively low and the time is short, the surface patches effect could not be regarded as the main factor to the enhancement of the barrier height.

When the sample was under illumination condition, the change of current was significant for annealed sample as compared to the as grown sample. Both as grown and annealed samples originated from the same AlGaN wafer, and both of the devices were fabricated using same processing tools and under identical parameters, however, significant difference in dark current was observed. High dark current in the as grown sample could be attributed to the low barrier height of the metal contact with the AlGaN thin film.

Since the Ni film became more transparent after annealing in O_2, more photons should be absorbed by the underneath semiconductor. The oxidation layer near the interface provides an increasing energy barrier for carrier injection into AlGaN. As the oxidation temperature increases (annealed at 800 ºC), the rectifying characteristics is deteriorated by excess oxidation. There may be some interfacial reaction between oxygen and AlGaN. The real interaction is still investigated.

The effect of the reduction of leakage current or dark current, barrier height or ideality factor enhancement in the MSM photodiodes after heat treatment can mainly be explained by the chemical reaction of the metal with the interfacial oxide layer of the semiconductor [15] or macroscopic interaction between the metal and the semiconductor [16]. Experimental results also show that reactive contact metals reduce the interfacial layer and react with the semiconductor during annealing and thus it can cause a low or high barrier height for MSM photodiodes.

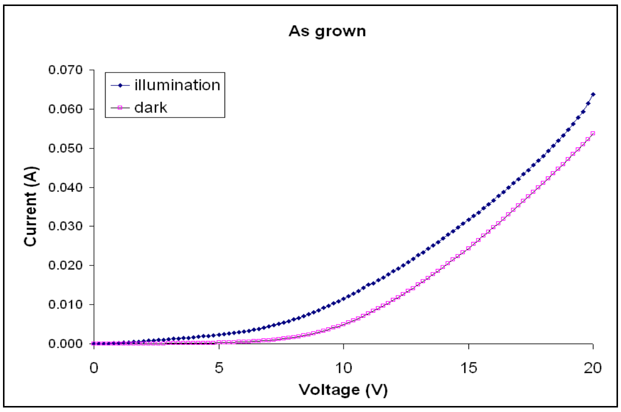

Fig. 2. Current-voltage (I-V) characteristics of the as grown samples.

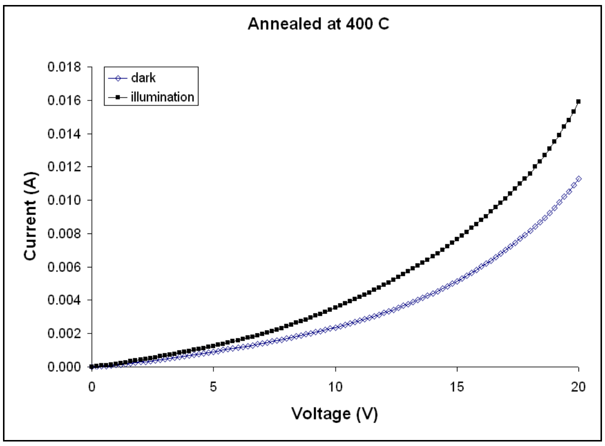

Fig. 3. Current-voltage (I-V) characteristics of the samples annealed at 400°C.

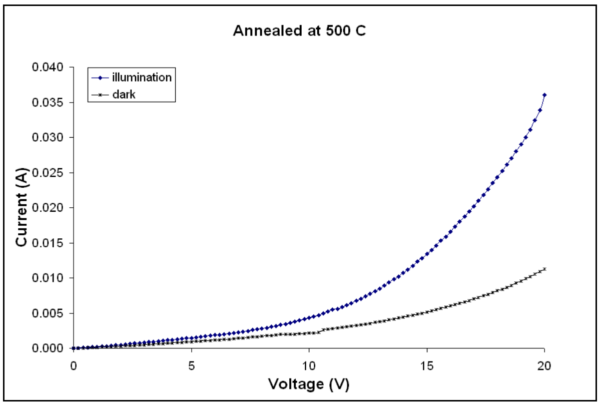

Fig. 4. Current-voltage (I-V) characteristics of the samples annealed at 500°C.

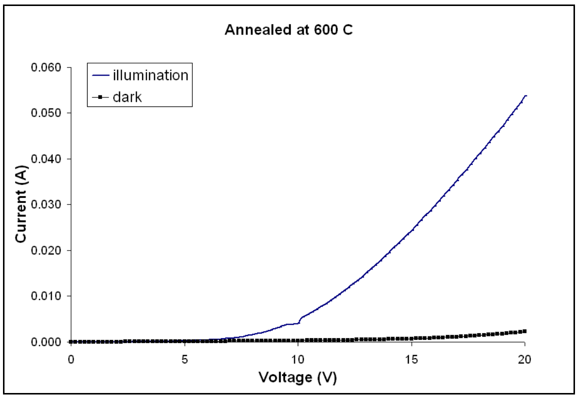

Fig. 5. Current-voltage (I-V) characteristics of the samples annealed at 600°C.

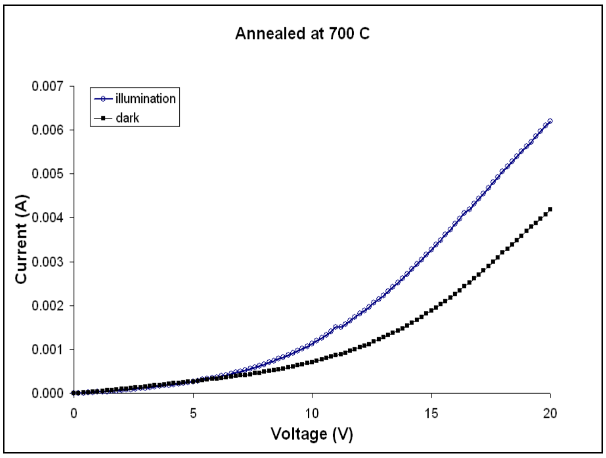

Fig. 6. Current-voltage (I-V) characteristics of the samples annealed at 700°C.

It can be seen that dark current rises slowly with the applied reverse bias and does not show any effect of saturation. The lack of saturation for a Schottky contact under reverse bias can be commonly explained in terms of barrier height is dependent on the electric field strength in the barrier as a result of the existence of an interfacial layer between the metal and the semiconductor. The lack of saturation can also be caused by image force lowering of the barrier height and due to the generation of electron-hole pairs in the depletion region as generation current is more pronounced at low temperatures than high temperatures because it has lower activation energy than the thermionic emission component [17].

Table 1. Summary of the dark current characteristics of the samples annealed in oxygen ambient at different temperatures.

Temperature (°C)	Samples (MSM photodiodes)	Ideality factor, n	Barrier height, Φ_b (eV)	Current at 10V (A)
As grown	illumination	1.23	0.51	1.15×10^{-2}
	dark	1.20	0.53	4.94×10^{-3}
400°C	illumination	1.15	0.55	3.54×10^{-3}
	dark	1.10	0.57	2.37×10^{-3}
500°C	illumination	1.09	0.60	4.29×10^{-3}
	dark	1.08	0.61	2.15×10^{-3}
600°C	illumination	1.05	066	4.04×10^{-3}
	dark	1.04	0.69	3.25×10^{-4}
700°C	illumination	1.02	0.67	1.13×10^{-3}
	dark	1.01	0.70	7.09×10^{-4}

$Al_{0.09}Ga_{0.91}N$ is known to suffer from a high amount of defect densities due to reasons like the difference between the thermal expansion coefficient and large lattice mismatch between the substrates and the $Al_{0.09}Ga_{0.91}N$ material, especially of those grown on Si. During the reverse bias of the Schottky contact, the effect of the applied bias can be much greater when compared to the forward bias. Thus, tunneling current can also be seen in a semiconductor with a lower doping concentration during reverse biases which indicate that the tunnel current cannot be omitted when are investigated Schottky contacts under reverse bias voltage.

Thus, apart from the usual thermionic emission current that exist within a metal-semiconductor contact, the high amount of dark current observed can be attributed to the tunneling of carriers across the barrier. This effect can be assisted by traps generated by defects (threading dislocations that reach the surface) and the interfacial layer to produce trap assisted tunnel currents. Deep level bulk states that are within a tunneling distance of the interface can be another kind of traps. Therefore, thermionic emission is the primary transport mechanism in theses MSM photodiodes.

Another contribution to the high dark current in $Al_{0.09}Ga_{0.91}N$ is dominated by other current mechanism like leakage current generated by a high defect density present in $Al_{0.09}Ga_{0.91}N$ as well as the traps assisted tunnel current. The high defect density in $Al_{0.09}Ga_{0.91}N$ justifies the presence of inhomogeneity at Schottky contacts, which causes a local enhancement of the tunnel current. The rotation of the layer during the growth and the different positions of the III-element sources could produce alloy inhomogeneities, as already reported.

From the results, the value of the ideality factor is quite near to unity, thus indicating the high quality

Schottky contact under investigation and the absence of a thick interfacial layer. However, the existence of a thin interfacial layer cannot be ruled out unless the semiconductor is cleaved in an ultra high vacuum (UHV) condition [18]. The variation in barrier height values may be due to formation of alloy, different thickness of interfacial layer present on the film, variation in surface roughness of samples used, defects present in films, presence of several transport mechanism, and the variations in the local stoichiometry [19].

As shown in Fig 7, the observation by SEM reveals mirror like surface for the as grown contacts. However, the contacts of all the samples started experiencing agglomeration at temperature in excess of 400°C. In our SEM surface images of the 600°C and 700°C samples shown in Fig. 7, both samples exhibit a “balling up” surface features, which is due to high temperature treatment. However, we can see that the annealed sample exhibits a rougher surface when compared to the as grown samples, where the sample exhibits a surface morphology with the absence of a wavy surface. AFM measurements are performed on the Schottky contact of the photodiodes to confirm the structural quality of the metal-semiconductor contact after treatment as shown in Table 2 and Fig. 8. All of the samples under annealing treatment have larger root mean square (rms) surface roughness than the as grown samples.

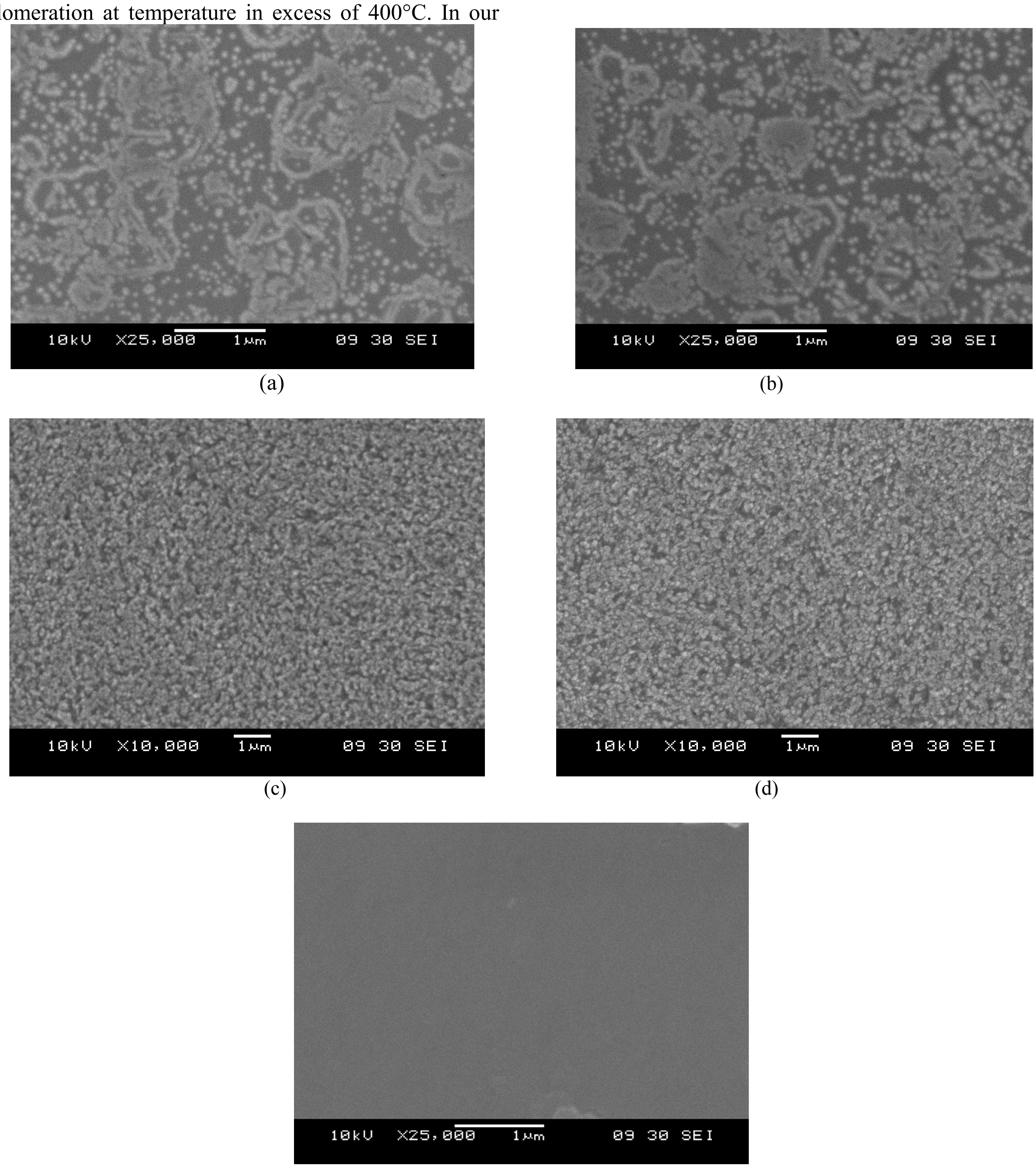

Fig. 7. Scanning electron microscopy image of the Ni Schottky contact on the AlGaN MSM photodiodes annealed at temperatures: (a) 400 °C, (b) 500 °C, (c) 600 °C, (d) 700 °C, and (d) as grown.

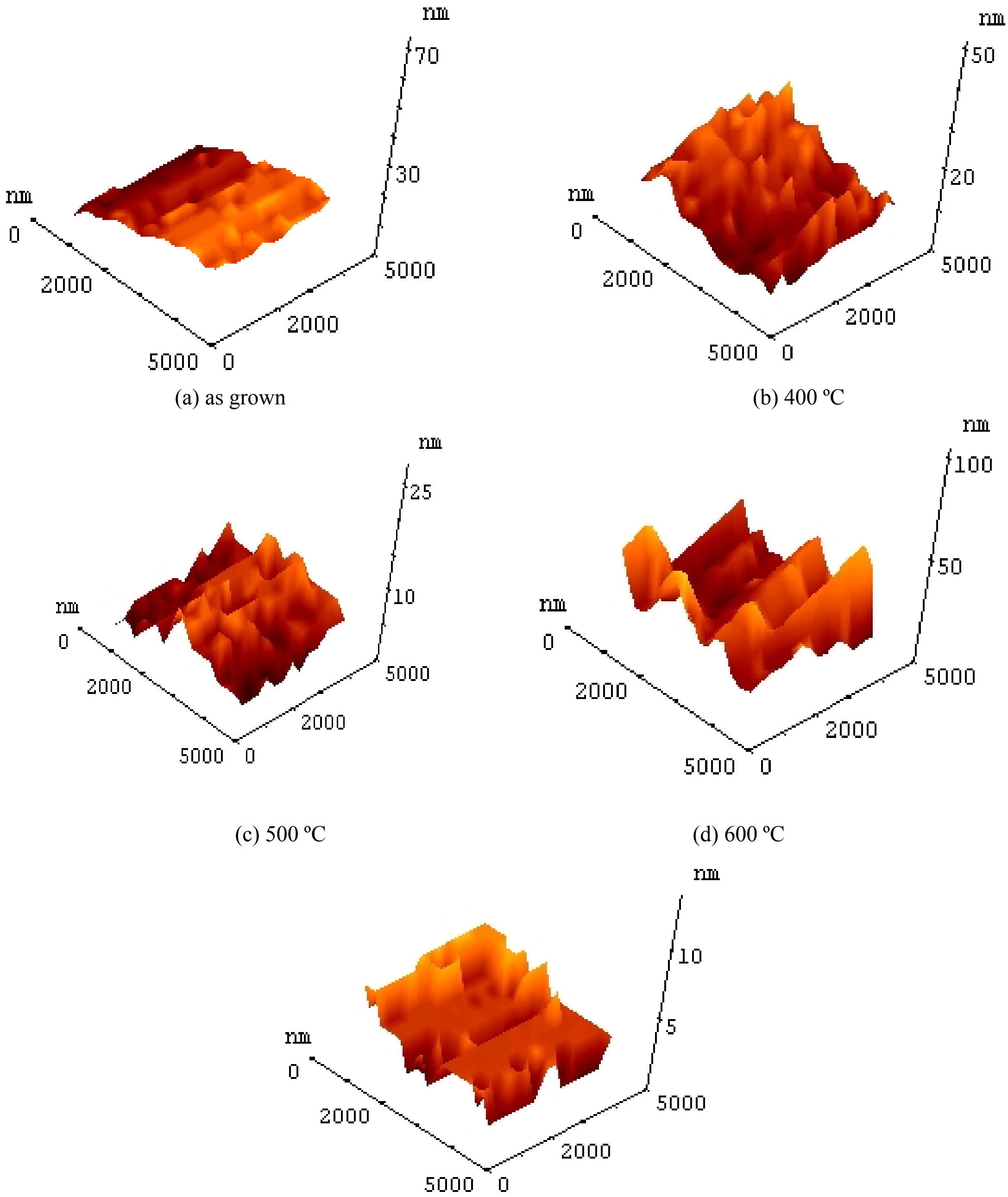

(a) as grown (b) 400 ºC

(c) 500 ºC (d) 600 ºC

(e) 700 ºC

Fig. 8. Atomic force microscopy images of the Ni Schottky contact on the AlGaN MSM photodiodes under annealed.

Table 2. AFM rms surface roughness values of the Schottky contacts for the samples annealed at different temperatures.

Temperature (°C)	AFM measurements, rms (nm)
400°C	10.02
500°C	11.30
600°C	12.41
700°C	13.47

The surface looks wavy due to the expansion or contraction of the metal (Ni) surface which generated the “black patches” as the Ni was moving away at different direction resulting in a wavy-like surface due to the generated “hillocks” at the metal surface. The expansion and contraction of Ni during heating and cooling will generate some compressive stress and strain to the metal surface due to the difference in thermal expansion coefficients between the AlGaN (α~5.6 ×10^{-6} K^{-1}) [20] and the Ni (α~13.4×10^{-6} K^{-1}) [21].

In the literature, Kang et al. presented that a NiO layer is easily formed when Ni is oxidized at temperature 300 ºC [22]. Therefore, in this work, the role of the post annealing in O_2 is considered to form a NiO layer on AlGaN. NiO is reported to behave as a p-type semiconductor with nickel vacancies and oxygen interstitials [23]. It is more insulating and transparent than Ni metal. Furthermore, NiO may induce passivation on the AlGaN interface [24]. It has been widely used in the GaN-based light emitting diodes (LEDs) as an ohmic contact to p-type GaN [25].

4. Conclusions

In conclusion, we have studied the effect of the post annealing in oxygen ambient to the Ni metal-semiconductor-metal (MSM) photodiode on AlGaN. The best Schottky contact is obtained when the annealing temperature is 700 ºC. The ideality factor is 1.01 for dark current and the barrier height is 0.70 eV. The mechanism of the barrier enhancement is explained with passivation effect due to the formation of NiO.

Acknowledgments

Financial support from FRGS grant and Fellowship from Universiti Sains Malaysia are gratefully acknowledged.

References

[1] J. I. Pankove: Mater. Res. Soc. Symp. Proc. **162**, 515 (1990).
[2] E. Monroy, F. Calle, E. Munoz, Appl. Phys. Lett., **74**(22), 3401 (1999).
[3] E. Monroy, F. Calle, J. L. Pau, E. Munoz, F. Omnes, B. Beaumont, P. Gibart, Journal of Crystal Growth **230**, 537 (2001).
[4] S. Averine, Y. C. Chan, Y. L. Lam, Appl. Phys. Lett., **77**(2), 274 (2000).
[5] V. L. Rideout, Solid-State Electron. **18**, 541 (1975).
[6] Abdulmecit Turut, Sebahattin Tuzemen, Muhammet Yildirim, Bahattin Abay, Mustafa Saglam, Solid-State Electron., **35**(10), 1423 (1992).
[7] P. Hacke, T. Detchprohm, K. Hiramatsu, N. Sawaki, Appl. Phys. Lett. **63**, 2676 (1993).
[8] K. Kim, W. R. L. Lambrecht, B. Segall, M. V. Schilfgaarde, Phys. Rev. **B 56**, 7363 (1997).
[9] Piotr Perlin, Tadeusz Suski, Michal Leszczynski, Henryk Teisseyre in *GaN and Related Materials*, edited by S. J. Pearton, (Gordon and Breach Science Publishers, Amsterdam, 1997).
[10] Q. Z. Liu, L. S. Yu, F. Deng, S. S. Lau, J. M. Redwing, J. Appl. Phys. **84**, 881 (1998).
[11] S. Averine, Y. C. Chan, Y. L. Lam, Appl. Phys. Lett., **77**(2), 274 (2000).
[12] L.C. Chen, F.R. Chen, J.J. Kai, J. Appl. Phys. **86**, 3826 (1999).
[13] H. Kim, M. Schuette, H. Jung, J.H. Song, J. Lee, W. Lu, Appl. Phys. Lett. **89**, 053516 (2006).
[14] T. Sawada, Y. Ito, K. Imai, K. Suzuki, H. Tomozawa, S. Sakai, Appl. Surf. Sci, **159/160**, 449 (2000).
[15] Abdulmecit Turut, Sebahattin Tuzemen, Muhammet Yildirim, Bahattin Abay, and Mustafa Saglam, Solid-State Electron., **35**(10), 1423 (1992).
[16] Q. Z. Liu, L. S. Yu, F. Deng, S. S. Lau, J. M. Redwing, J. Appl. Phys. **84**, 881 (1998).
[17] E. H. Rhoderick, R. H. Williams, Metal-Semiconductor Contacts, second ed., (Oxford University Press, New York, 1988), p. 132.
[18] J. D. Guo, F. M. Pan, M. S. Feng, R. J. Guo, P. F. Chou, C. Y. Chang, J. Appl. Phys. **80**(3), 1623 (1996).
[19] S. J. Pearton, J. C. Zolper, R. J. Shul, F. Ren, J. Appl. Phys, **86**(1), 1 (1999).
[20] Jung Han, M. H. Crawford, R. J. Shul, S. J. Hearne, E. Chason, J. J. Figiel, M. Banas, MRS Internet J. Nitride Semicond. Res. **4S1**, G7.7 (1999).
[21] G. W. C. Kaye, T. H. Laby, Tables of Physical and Chemical Constants, (Longman, Essex, 16th ed., 1995), p.73.
[22] H.C. Kang, S.H. Seo, H.W. Jang, Appl. Phys. Lett. **83,** 2139 (2003).
[23] L.C. Chen, F.R. Chen, J.J. Kai, J. Appl. Phys. **86,** 3826 (1999).
[24] H. Kim, M. Schuette, H. Jung, J.H. Song, J. Lee, W. Lu, Appl. Phys. Lett. **89,** 053516 (2006).
[25] C.Y. Hu, Z.X. Qin, Z.X. Feng, Z. Z. Chen, H. Yang, Z.J. Yang, T.J. Yu, X.D. Hu, S.D. Yao, G.Y. Zhang, Chin. J. Semiconduct. **26**, 1154 (2005) (in chinese).

*Corresponding author: chuahleesiang@yahoo.com